CONF-900505--10

CONF-900505--10

DE91 004429

Modeling and Analysis of Surface Roughness Effects on Sputtering, Reflection, and Sputtered Particle Transport*

J.N. Brooks
Argonne National Laboratory, Argonne, IL, USA

and

D.N. Ruzic
University of Illinois, Urbana, IL, USA

DISCLAIMER

---

*Work supported by the U.S. Department of Energy, Office of Fusion Energy.

Manuscript submitted to the 9th International Conference on Plasma Surface Interactions in Controlled Fusion Devices, Bournemouth, UK, May 20-25, 1990.

Modeling and Analysis of Surface Roughness Effects on Sputtering, Reflection, and Sputtered Particle Transport*

J.N. Brooks
Argonne National Laboratory, Argonne, IL, USA

and

D.N. Ruzic
University of Illinois, Urbana, IL, USA

Abstract

The microstructure of the redeposited surface in tokamaks may affect sputtering and reflection properties and subsequent particle transport. This subject has been studied numerically using coupled models/codes for near-surface plasma particle kinetic transport (WBC code) and rough surface sputtering (fractal-TRIM). The coupled codes provide an overall Monte Carlo calculation of the sputtering cascade resulting from an initial flux of hydrogen ions. Beryllium, carbon, and tungsten surfaces are analyzed for typical high recycling, oblique magnetic field, divertor conditions. Significant variations in computed sputtering rates are found with surface roughness. Beryllium exhibits high D-T and self-sputtering coefficients for the plasma regime studied (T_e = 30-75 eV). Carbon and tungsten sputtering is significantly lower.

---

*Work supported by the U.S. Department of Energy, Office of Fusion Energy.

Introduction

Fusion surface erosion may depend on surface microstructure via changes in sputtered particle velocity distributions and by overall sputtering coefficients. This may be particularly true for a high redeposition plasma regime where near-surface impurity transport is important. A recent study examined sputtered impurity transport for high recycle, oblique magnetic field, tokamak divertor conditions [1]. The study used the WBC Monte Carlo code to compute the sub-gyro orbit motion of the particles in a fixed background D-T plasma. This work focused on modeling of plasma-impurity interactions, and treated the surface sputtering using analytical models appropriate for smooth surfaces. In the area of surface modeling, recent work has been done on modeling sputtering from rough surfaces by using fractal geometry in the TRIM binary collision code [2-3]. For this paper these codes, WBC and FTRIM, have been coupled to provide a more self-consistent calculation of the effects of microstructure on sputtering and transport, for typical high recycle divertor conditions. General goals of this work are to check on previous (favorable) self-sputtering results for tungsten [1] and to provide estimates of D-T and self-sputtering coefficients for beryllium and carbon, for high recycling divertor conditions.

Computational Model

Figure 1 shows the model geometry. The (net) magnetic field lies in the z-y plane and is uniform in the x-direction. The plasma has a uniform temperature, $T_e = T_i$, sound speed flow (prior to the sheath), and electron density prior to the sheath $N_e = N_{e_o}$. The sheath potential is modeled, based on considerations summarized in ref. 1, with the following dual structure:

$$\phi(z) = \phi_1 \exp(-z/2\lambda_D) + \phi_2 \exp(- z/R_{DT})$$

where $\phi_1 + \phi_2 = \phi_0$ is the total sheath potential, λ_D is the Debye length at the start of the sheath, and R_{DT} is the D-T ion gyroradius. The electron density in the sheath is given as:

$$N_e = N_{e_o} \exp(e\phi/kT_e).$$

The following parameters are used in the calculations; $\psi = 87°$, B = 5T,

$N_{e_o} = 1 \times 10^{20}$ m^{-3}, $e\phi_o/kT_e = 3$. Values of ϕ_1 and ϕ_2 are used such that 25% of the total sheath potential difference occurs in the Debye sheath region, $0 \leq Z \lesssim 6\ \lambda_D$, and 75% occurs in the magnetic sheath, $6\lambda_D \lesssim Z \lesssim 3R_{DT}$.

Impurity transport is treated by first computing the sputtering from an impinging current of D-T ions, and then following the resulting self-sputtering cascade arising from the redeposited impurities. For beryllium and carbon surfaces the FTRIM code was used to compute an array of sputtered atom launch velocities, $\bar{V}$, for 2000-10,000 incident D-T ions, for T_e = 30, 75 eV, and for a range of fractal dimensions D. The impinging D-T ion velocities were chosen from a distribution with mono-energetic energy of $U_{DT} = 5\ kT_e$, a normal distribution in elevation angle with mean $\bar{\theta}_{DT} = 65°$ and a standard deviation of 10°, and a fixed azimuthal angle of $\Phi = 68°$. These values are based on typical calculated results for oblique incidence field geometries [4-6].

The atomic-scale fractal dimension of a surface can be measured by gas adsorption techniques. Surface roughness factors have been found this way [7] for fusion related materials. However, those experiments used just one size of adsorbed gas atom to make the measurements. By using a variety of adsorbate sizes a fractal dimension can be found. By using such a technique graphite has been shown to have fractal characteristics on the few to 100s Å scale ranging from a fractal dimension D of approximately 2.05 to 2.30 [8]. A range of D from 2.01 (very smooth surface) to 2.50 (very rough) was adopted for this work. (Values of D > 2.3 are probably non-physical but are included to show trends.)

The D-T sputtering results are discussed in the following section. For tungsten, the D-T sputtering coefficient is too low to make the above procedure practical. Instead, a D-T sputtered array was generated assuming a constant W^o launch energy of $U_o = \frac{1}{2} U_B$, for a binding energy U_B = 11.1 eV, and using probability distribution functions $f_1(\theta) = 2 \cos\theta \sin\theta$, and $f_2(\Phi) = \frac{1}{2\pi}$. This array for tungsten also simulates sputtering by other low-Z plasma ions, notably, He^{+2}.

To compute self-sputtering, a (variable) number of the impurity atoms from the D-T sputter array is launched. Transport of these particles in the plasma is followed by the WBC code [1]. The WBC code computes impurity transport due to charge changing and velocity changing collisions with the plasma, and the Lorentz force motion due to the electric and

magnetic fields. If an impurity ion is redeposited, which almost all are in the regime studied, the particle velocity is used as input to FTRIM. The resulting reflected particle, if any, and any sputtered particles are then launched and followed by WBC. This procedure is iterated to follow a complete cascade from the D-T and self-sputtered atoms.

D-T Sputtering Results

Figure 2 shows the calculated D-T sputtering coefficient for beryllium and carbon, for the conditions mentioned. For each case, 10,000 flights were run for D-T on C, 2500 for D-T on Be at U_{DT} = 150 eV (T_e = 30 eV), and 2000 for D-T on Be at U_{DT} = 375 eV (T_e = 75 eV). Statistical errors are in the range of 3-5% for these cases.

As shown, increasing surface roughness decreases the D-T sputtering coefficient. It should be noted, however, that the yield for a case of D = 2.01 is greater than that predicted for an atomically smooth surface with D = 2.00 [3]. Although some degree of surface roughness allows primary knock-ons to become sputtered atoms directly without having to suffer any additional collisions, this is overcome by other potentially sputtered particles being captured by surface features as the surface roughness is increased.

A typical energy distribution of D-T sputtered particles is shown in fig. 3. The energy distribution is not a significant function of surface roughness. For most cases the angular distribution is also independent of surface roughness and is cosine in nature. However, for the smallest incident/target mass ratio, i.e., D-T → C an angular dependence on fractal dimension is evident. Figure 4 (a and b) shows the elevation and azimuthal angular dependence respectively for the sputtered atoms at three degrees of surface roughness. For the smoothest case, the sputtered particles are peaked in the direction of the incident ion and come off at shallow elevation angles. As the roughness is increased the distribution becomes a cosine distribution and looses its azimuthal dependence.

Self-Sputtering Results

Coupled computer code simulations were made as described above, to compute the D-T and self-sputtering cascades. For each case a total of 600 sputtered particle histories were computed, with additional runs made to assess variances. (Because of differences in sputtering coefficients,

each case involves a different mix of D-T sputtered and self-sputtered particles.) The non-vectorized coupled codes proved to be quite time consuming, with each particle history taking about 0.5 S CPU time on a CRAY2. We hope to speed this up in the future.

Table 1 lists values of some key impurity transport parameters, for a typical value of D = 2.1. In general, the average redeposited elevation angle, and charge state is fairly constant with D, while the average sputtered energy (not listed) and redeposited energy tend to increase somewhat with increasing roughness. As implied by the large variances in transit time there is a small but significant fraction of particles taking much longer than the average to be redeposited. This arises due to the impurity/plasma collision scaling properties. As was found in an earlier study [1] sputtered carbon, and in this case also beryllium, tends to be ionized outside of the sheath (approximate width $3R_{DT} \approx 0.5$ mm, at T_e = 30 eV) while tungsten, on average, is ionized within the sheath. The inclusion of D-T sputtered particle transport, in the present work, tends to lower the average charge state for tungsten, compared to previous, self-sputtering only, results [1]. In general, redeposited charge states are all much lower than the coronal equilibrium values.

Figures 5-6 show the average self-sputtering coefficient, $\bar{Y}_{Z-Z}$, for the cases ran. This is defined as: $\bar{Y}_{Z-Z}$ = (sputtered + reflected impurity atoms)/(incident impurity ions). Statistical error in $\bar{Y}_{Z-Z}$ was found to be about 6% for the cases checked. For both values of T_e there is a minimum in self-sputtering coefficient, at low values of fractal dimension. Unlike light-atom sputtering, a great deal of energy can be transferred in a self-sputtering collision. If one of these higher energy sputtered particles strikes additional surface features on its way out of the surface, additional sputtered atoms can be created. This effect increases the sputtering yield at intermediate degrees of surface roughness compared to the light atom sputtering results.

In general, beryllium exhibits a close-to-unity self-sputtering coefficient at both temperatures even for smooth surfaces. This is similar to computational results found by Roth [9] using an *a priori* specification of oblique incidence impinging beryllium ion velocities. Carbon and tungsten appear substantially better at T_e = 30 eV, and at T_e = 75 eV as well, except for high and probably non-physical values of surface roughness, D = 2.5.

Conclusions

This work has examined surface roughness effects on sputtering and impurity transport for a divertor regime with 30-75 eV plasma temperatures at the sheath. The coupled computer codes used provide a self-consistent calculation of sputtering via the exchange of information about sputtered/redeposited particle velocities. The results indicate that surface roughness can play a significant role in determining erosion rates. A small degree of roughness, for example, decreases the computed D-T sputtering coefficient for carbon by ~40%, for T_e = 75 eV. Self-sputtering coefficients also can vary substantially with roughness, this is particularly important for values near unity.

Transport statistics of the combined D-T and self-sputtered impurity cascade were computed for the beryllium, carbon, and tungsten simulations. As seen in several previous studies, the low-Z materials exhibit off-normal redeposited incidence ($\bar{\theta} \approx 40\text{-}50°$) whereas tungsten tends to impact at more normal incidence. Sputtered carbon and beryllium tend to be ionized outside of the sheath and depend, for the most part, on plasma collisions to be redeposited, whereas tungsten tends to be redeposited much faster due to sheath electric field acceleration.

In general the sputtering results for beryllium appear discouraging, with high D-T and self-sputtering coefficients predicted at all values of fractal dimension D. There is, however, a roughness regime (D ≈ 2.1) where beryllium sputtering would be minimized. Carbon appears to offer much better sputtering erosion performance than beryllium. The present results for tungsten are encouraging, implying stable ($\bar{Y}_{Z\rightarrow Z} < 1$) operation for T_e = 75 eV, for physically plausible values of surface roughness. This supports earlier results [1] which used a simpler sputtering-model (but examined the plasma operating regime in much more detail).

These conclusions are subject to numerous uncertainties in the models used, e.g., in plasma collision terms, sheath structure, and limitations in the binary collision methodology of the TRIM code. Experimental data needed for code verification is, for the most part, lacking. Experiments to measure the fractal dimension of the atomic scale roughness are possible, and would appear to be desirable, in view of the trends shown here.

Acknowledgments

We would like to thank the Max-Planck-Institut für Plasmaphysik for permission to use the TRIM code, and the National Center for Supercomputing Applications at the University of Illinois for computational support.

References

[1] J.N. Brooks, Near-surface sputtered particle transport for an oblique incidence magnetic field plasma, Phys. Fluids, to be published.

[2] D.N. Ruzic and H.K. Chiu, J. Nucl. Mater. 162-164 (1989) 904.

[3] D.N. Ruzic, Nucl. Instrum. & Methods B47 (1990) 118.

[4] R. Chodura, J. Nucl. Mater. 111&112 (1982) 420.

[5] R. Chodura, Physics of plasma-wall interactions in controlled fusion, D.E. Post and R. Behrish editors (Plenum Publishing, New York, 1986).

[6] A.B. Dewald, A.W. Bailey, and J.N. Brooks, Phys. Fluids 30 (1987) 267.

[7] K. Nakayama, S. Fukuda, T. Hino, T. Yamachina, J. Nucl. Mater. 145-147 (1987) 301.

[8] D. Avnir, D. Farin, and P. Pfeifer, J. Chem. Phys. 79 (1983) 3556.

[9] J. Roth, W. Eckstein, and J. Bohdansky, J. Nucl. Mater. 165 (1989) 199.

Table 1. Impurity transport parameters for D = 2.1.

Parameter*		T_e = 30 eV			T_e = 75 eV		
		Be	C	W	Be	C	W
Neutral ionization distance (perpendicular to surface)	$\bar{Z}_o$	2.0 mm	2.3 mm	0.27 mm	1.7 mm	2.0 mm	0.33 mm
Transit time**	$\bar{\tau}$	3.0 μs	3.0 μs	0.41 μs	3.4 μs	3.6 μs	0.39 μs
	τ_{SD}	3.9 μs	3.7 μs	1.0 μs	7.8 μs	6.3 μs	1.4 μs
Elevation angle†	$\bar{\theta}$	48°	48°	18°	40°	44°	15°
	θ_{SD}	15°	14°	12°	17°	17°	12°
Charge state†	$\bar{K}$	1.6	2.0	2.1	1.5	2.2	2.2
	K_{SD}	0.48	0.82	1.4	0.50	1.2	2.1
Energy†	$\bar{U}$	188 eV	233 eV	184 eV	339 eV	564 eV	442 eV
	U_{SD}	91 eV	125 eV	211 eV	175 eV	386 eV	687 eV

*Bar denotes average value, SD denotes standard deviation.
**From first ionization until redeposition.
†Of redeposited ions.

FIGURE CAPTIONS

Fig. 1. Model geometry.

Fig. 2. D-T sputtering coefficients for beryllium and carbon as a function of fractal dimension.

Fig. 3. Energy distribution of D-T sputtered carbon, for T_e = 30 eV, D = 2.05.

Fig. 4 (a,b). Angular distributions of D-T sputtered carbon, for T_e = 30 eV, D = 2.01, 2.05, 2.5.

Fig. 5. Self-sputtering coefficients for beryllium, carbon, and tungsten, as a function of fractal dimension, for T_e = 30 eV.

Fig. 6. Self-sputtering coefficients for beryllium, carbon, and tungsten as a function of fractal dimension, for T_e = 75 eV.

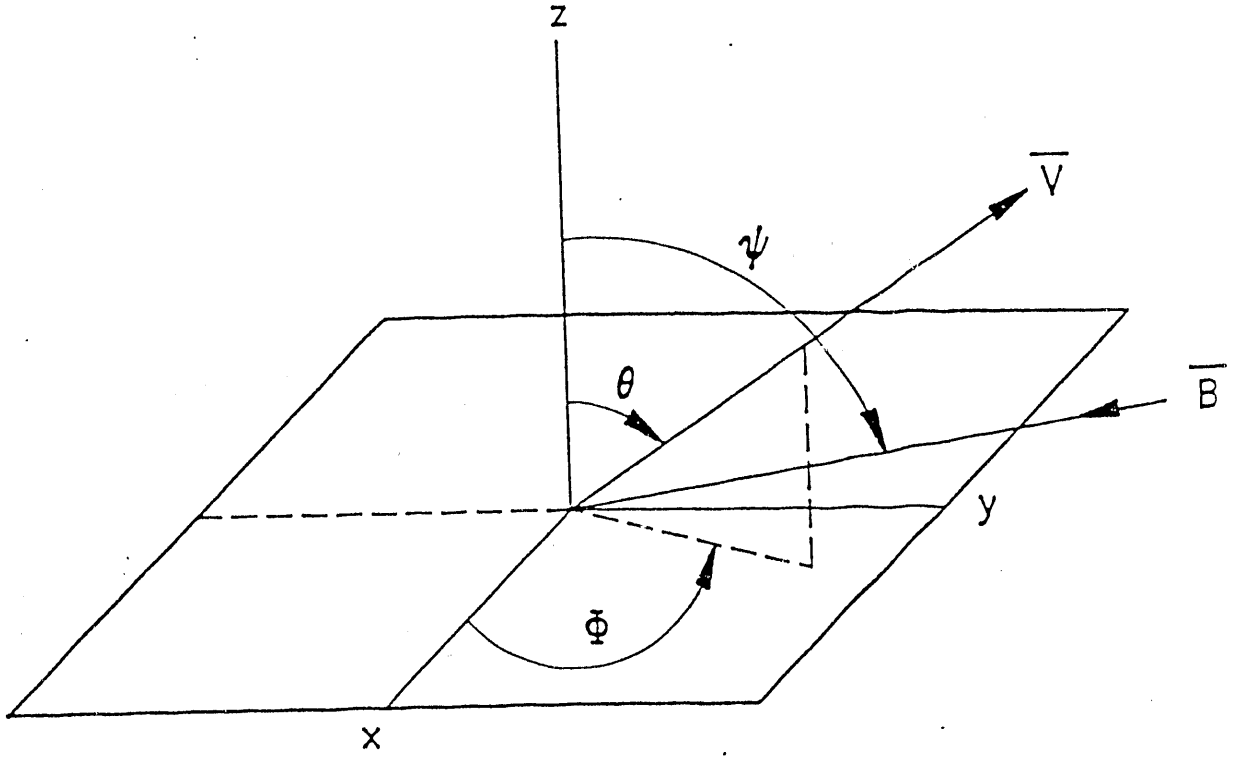

Fig. 1. Model geometry.

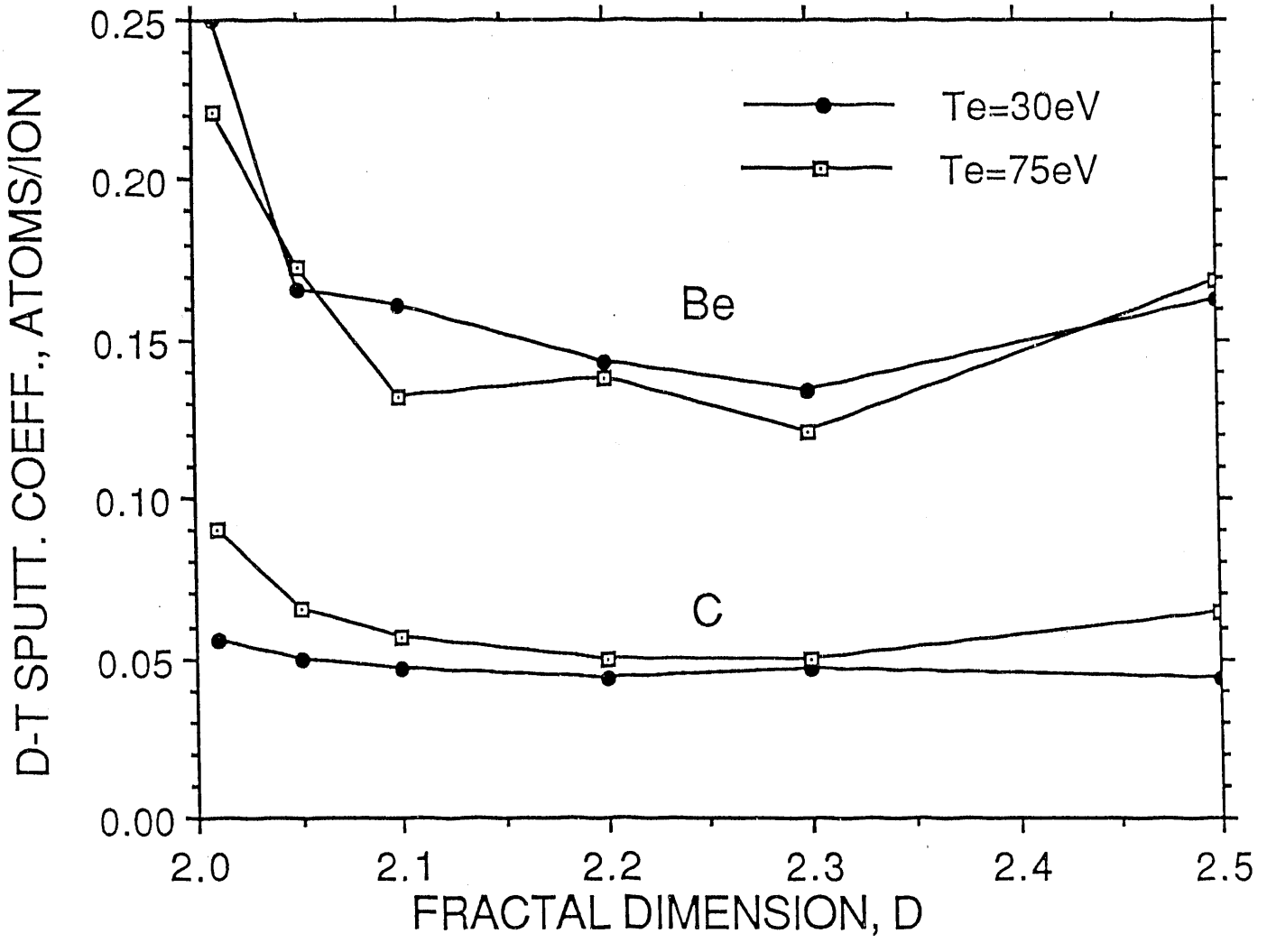

Fig. 2. D-T sputtering coefficients for beryllium and carbon as a function of fractal dimension.

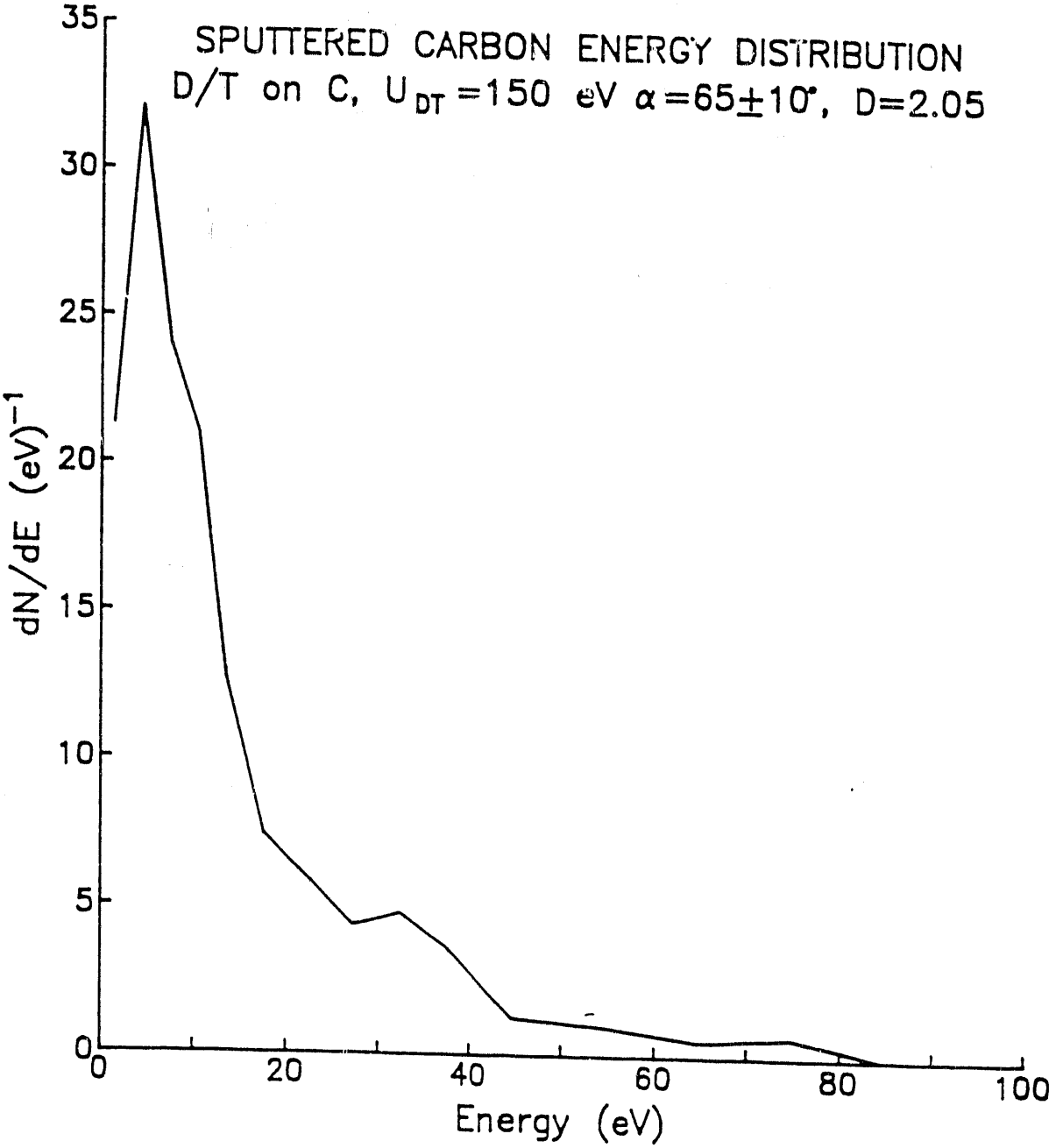

Fig. 3. Energy distribution of D-T sputtered carbon, for T_e = 30 eV, D = 2.05.

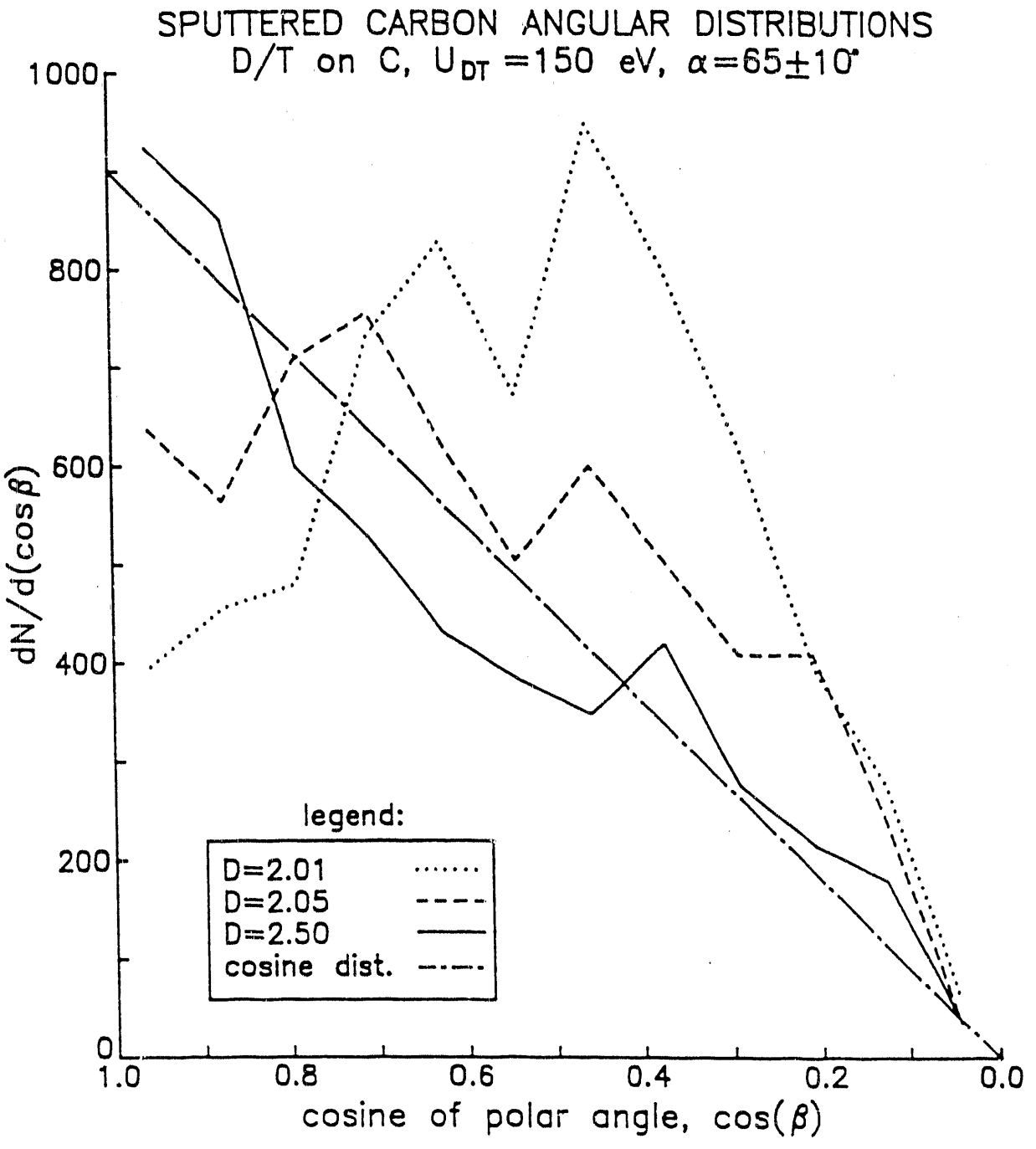

Fig. 4 (a,b). Angular distributions of D-T sputtered carbon, for T_e = 30 eV, D = 2.01, 2.05, 2.5.

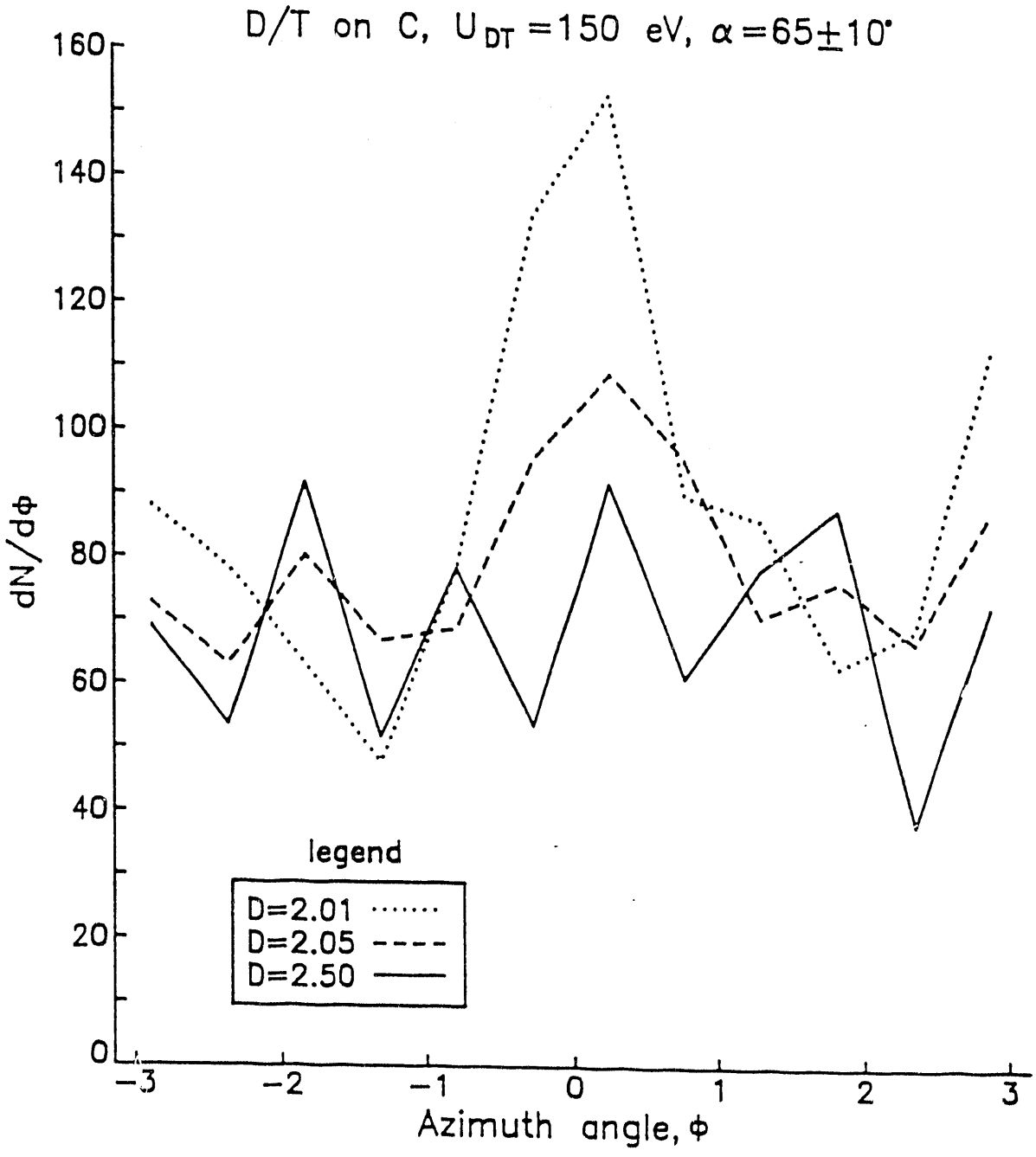
D/T on C, U_{DT} =150 eV, α=65±10°
dN/dΦ
160
140
120
100
80
60
40
20
0
−3
−2
−1
0
1
2
3
Azimuth angle, Φ
legend
D=2.01
D=2.05
D=2.50

Figure 4b

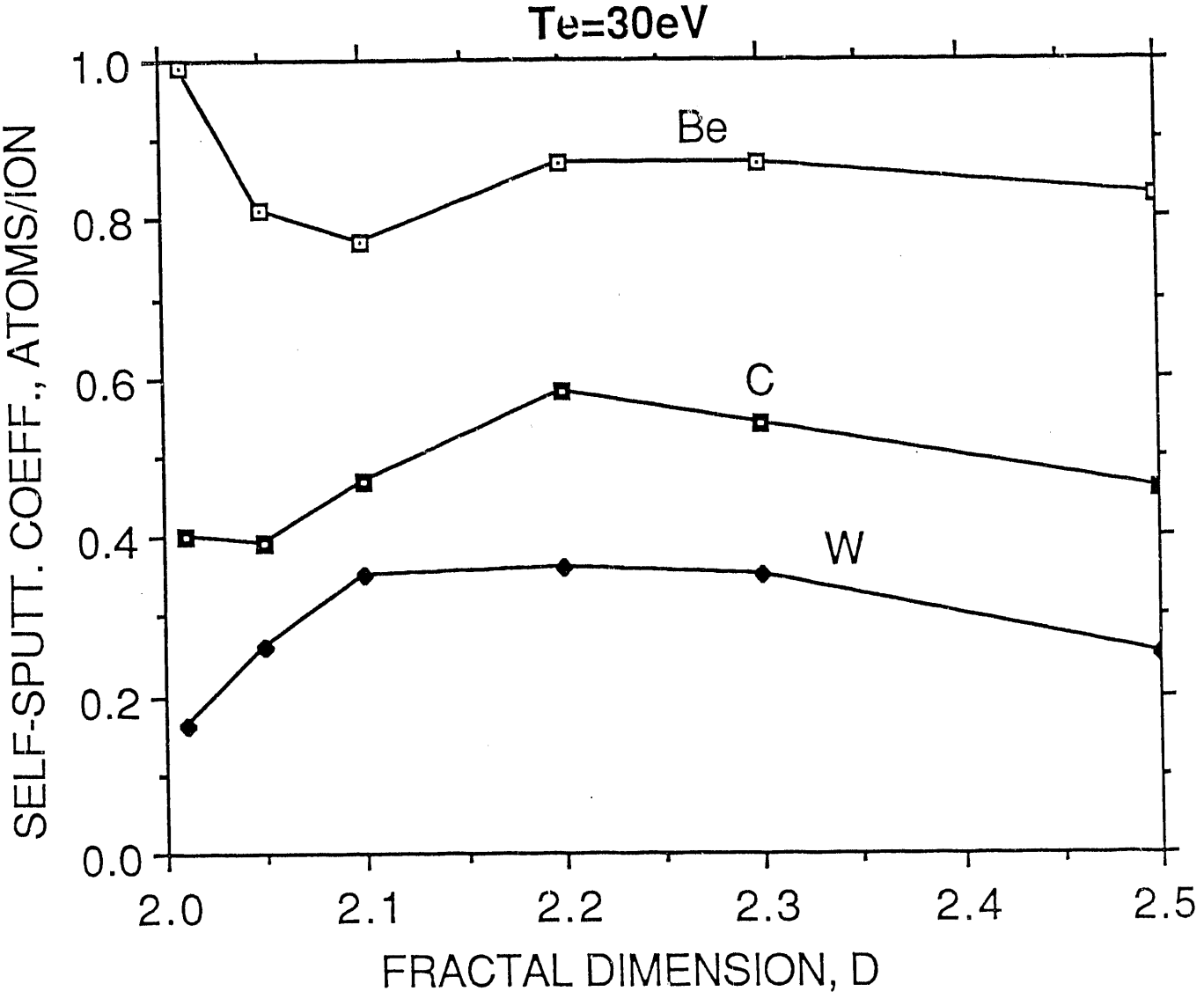

Fig. 5. Self-sputtering coefficients for beryllium, carbon, and tungsten, as a function of fractal dimension, for T_e = 30 eV.

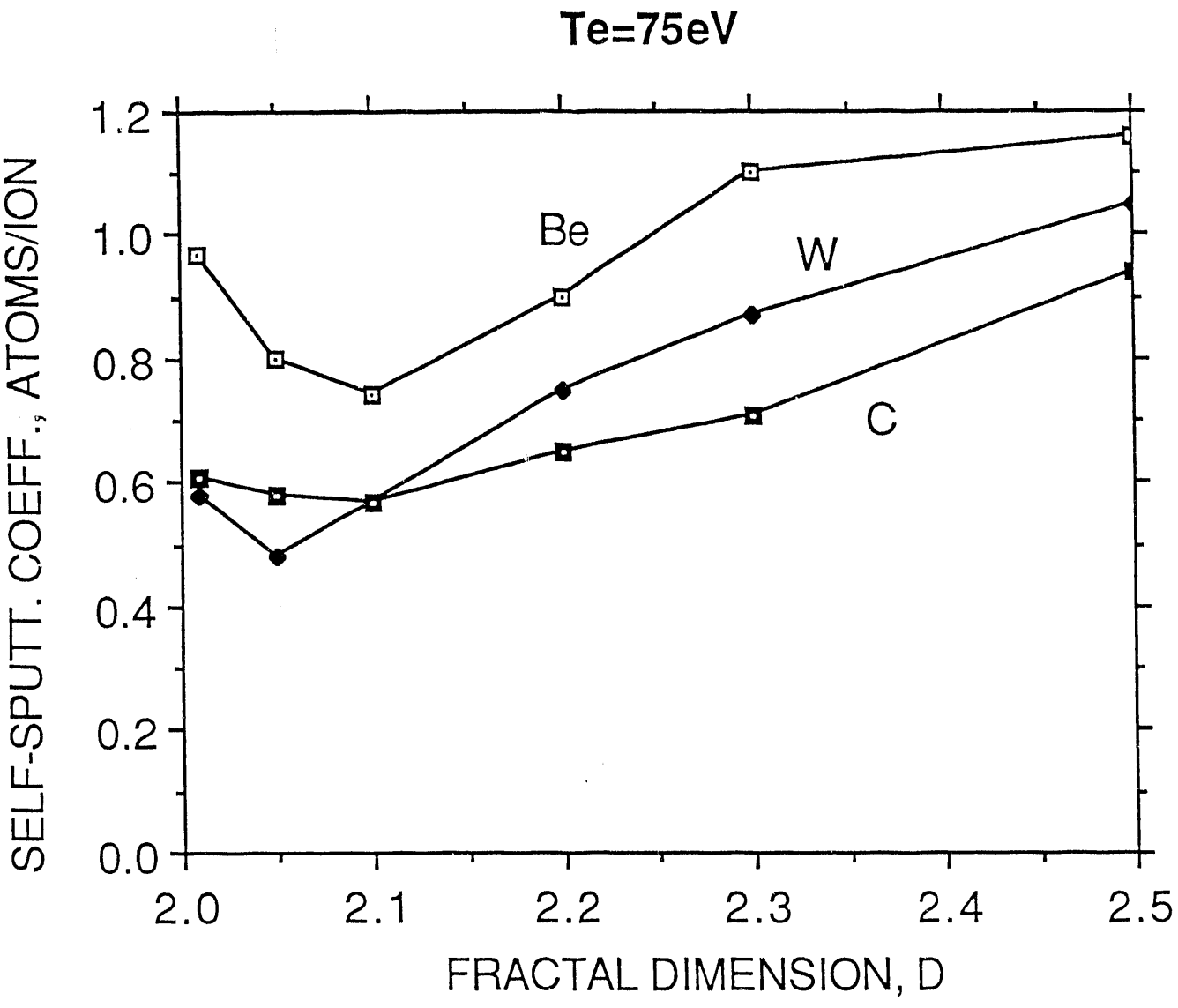

Fig. 6. Self-sputtering coefficients for beryllium, carbon, and tungsten as a function of fractal dimension, for T_e = 75 eV.

END

DATE FILMED

12/12/90